



## Dielectric Relaxation Behaviour and AC Electrical Conductivity of Cellulose Acetate-Molybdenum Trioxide Nanoparticle Blended Film



CrossMark

Dina Ezzat,<sup>a,\*</sup>, Mortada Youssif,<sup>b</sup>, Hanan Elhaes,<sup>a</sup> Mahmoud El-Nahass,<sup>c</sup>

<sup>a</sup>Physics Department, Faculty of Women for Arts, Science, and Education, Ain Shams University, 11757 Cairo, Egypt

<sup>b</sup> Physics Department, Faculty of Science at New Damietta, Damietta University, New Damietta 34517, Egypt

<sup>c</sup> Physics Department, Faculty of Education, Ain Shams University, Roxy, Cairo, Egypt

### Abstract

Cellulose acetate (CA) and CA blended with molybdenum trioxide MoO<sub>3</sub> nanoparticle at concentration of (0.0, 0.25, 0.5 & 1.0 wt. %) prepared by casting method. Ac conductivity and dielectric properties were studied. Our results indicated that the conduction mechanism of CA and CA blended with different concentration of MoO<sub>3</sub> nanoparticle is controlled by the correlation barrier hopping (CBH) model. The ac conductivity was observed to increase by adding MoO<sub>3</sub> nanoparticle which explained by the network formed as the nanoparticle gets closer to each other as the concentration increase. The maximum barrier height was calculated and found to decrease by increasing MoO<sub>3</sub> nanoparticle from 0.15 to 0.12 eV. The analysis of the dielectric constant and dielectric loss suggested that their behavior can be explained by Maxwell–Wagner–Sillar type polarization at high frequency. At low frequency the polarization is high as a result of interfacial polarization. Arrhenius equation was used to calculate the activation energy of relaxation which found to decrease by increasing MoO<sub>3</sub> nanoparticle.

**Keywords:** Cellulose Acetate; MoO<sub>3</sub>; Ac conductivity; Nanoparticle; Dielectric properties.

### 1. Introduction

The blending of different polymers is one of the most important ways to design a material with a wide variety of characteristics [1]. CA own potential compatibility, good dielectric constant and have excellent optical and mechanical properties. CA is used to manufacture fibers, films, laminates, adhesives, coatings, plastic products, and tactile actuators [2- 4]. The implementation of nanoparticles inside the polymer matrix has proved to be very helpful in manipulating different morphological, physical, and chemical properties in the way of supporting industrial applications. Blending polymer with transition metal oxide nanoparticles enhancing its

properties remarkably. These materials are good for applications in industry as catalysts, sensors, lubricants, display devices, smart windows, battery electrodes, etc. [5-8]. MoO<sub>3</sub> is an n-type semiconductor transition metal oxide which have a band gap of 3.15 eV. It has a wide range of applications such as in smart windows, gas sensors, imaging devices, electrochromism, photochromism, , electrocatalysis, heterogeneous catalysis, , field-effect transistors, electrodes of rechargeable batteries, and supported catalysts [9, 10]. Dielectric studies in relation to polymer films are of special interest because of their possible technical applications for insulation, isolation, and passivation in microelectronic circuits. The dependence of the dielectric properties on temperature and frequency give precious data on the chemical and physical state

\*Corresponding author e-mail: [dandona.phy@hotmail.com](mailto:dandona.phy@hotmail.com).; (Dina Ezzat).

Receive Date: 30 December 2020, Accept Date: 15 January 2021

DOI: 10.21608/EJCHEM.2021.55850.3181

©2021 National Information and Documentation Center (NIDOC)

of the polymer [1]. Ac and dielectric properties for thin film of pure CA and CA with different concentration of erbium (III) chloride ( $\text{ErCl}_3$ ) were studied and reveal that Correlated barrier hopping model was the dominant mechanism for study pure CA [12]. Influence of iron doping and its concentration on the dielectric characteristic of cellulose acetate films was studied. Doping with Fe was observed to decrease the dielectric capacitance as well as the dielectric loss was observed to increase by doping CA with Fe [13]. Molybdenum trioxide nanoparticle with different concentration was used in blending PVA/PVP polymer nanocomposites and it was seen that the dielectric and electrical properties were improved with the addition of  $\text{MoO}_3$ -nanoparticle (NPs) [14]. Accordingly, the present study introduces the influence of blending CA with various concentrations of  $\text{MoO}_3$ -NPs on ac conductivity and dielectric properties of pure CA as a function of frequency and temperature. The dielectric study of the blending is an important step toward further application of this important material.

## 2. Experimental

CA and  $\text{MoO}_3$ -NPs were purchased from Aldrich company, Inc., USA. Cellulose acetate with 39.7 wt.% acetyl content. Meanwhile, dimethyl sulphoxide was purchased from Labscan Ltd., Unit. However, CA and CA/ $\text{MoO}_3$ -NPs blend materials were prepared by previously used casting technique [15]. Where, 1g of CA powder was dissolved in 20ml of Dimethyl Sulphoxide with  $\text{MoO}_3$ -NPs with concentrations varying of (0.0, 0.25, 0.5 and 1.0 wt %). The solution was then stirred under a fixed mechanical stirring with a moderate speed of spin for about two hours at  $40^\circ\text{C}$  with continuous stirring in the way to form a homogeneous solution and to assure that CA was completely dissolved. The blended solutions were casted carefully on glass plates and placed on a table waiting for about two hours in air to get rid of the air bubbles. The casting solution was then placed in a dryer at  $60^\circ\text{C}$  for about three days to be dried. Then the dried samples were carefully taken off from the glass plates using a sharp knife. AC electrical measurements were performed by using a programmable automatic LCR Bridge (model Hioki 3532-50 Hi-tester) in the frequency range of 42 HZ to 5MHz. The sample was placed in a gold holder specially designed to minimize stray capacitance. The

temperature of the sample was measured by a thermocouple over a temperature range of 313 to 373 K. For the sample under investigation, the impedance,  $Z$ , the capacitance,  $C$ , and the phase angle,  $\phi$ , were measured directly. The total conductivity was calculated from the following equation:  $\sigma(\omega, T) = d/ZA_0$ , where  $d$  is the thickness of the sample and  $A_0$  is the cross-section area. The dielectric constant,  $\epsilon'(\omega)$ , was calculated from the equation:  $\epsilon'(\omega) = dC/A\epsilon_0$ , where  $\epsilon_0$  is the permittivity of free space. The dielectric loss,  $\epsilon''(\omega)$ , was calculated from the equation:  $\epsilon'' = \epsilon' \tan \delta$ , where  $\delta = 90 - \phi$  [16].

## 3. Results and Discussions

Electrical conductivity is a prominent factor which gives reliable data about the transport phenomenon in materials. Figure 1 (a, b, c & d) shows the natural logarithm of the total electrical conductivity  $\sigma(\omega, T)$  vs.  $\ln(\omega)$  at different temperatures for CA blended with different concentration of  $\text{MoO}_3$ -NPs. The figures indicate the typical characteristic of many solids (semiconductors, glasses, ionic conductors and organic materials) where  $\sigma(\omega, T)$  is approximately practically constant at low frequency and after a specific frequency, it increases with power law by increasing the frequency. The  $\sigma(\omega, T)$  for CA with different concentration of  $\text{MoO}_3$ -NPs. can be studied under the consideration of Jonscher's universal dispersion relaxation (Jonscher's UDR) mathematical expression [16, 17, 18]:

$$\Sigma(\omega, t) = \sigma_{dc}(0, t) + \sigma_{ac}(\omega, t) = \sigma_{dc}(t) + A\omega^s \quad (1)$$

where  $\sigma_{dc}(T)$  is the DC conductivity which is resulted by the long-range motion of electrical charge carriers which is independent of frequency and dependent on temperature and determined from the interception of the curve of the total conductivity with y-axis,  $\sigma_{ac}$  is the ac conductivity is resulted by the relaxation or polarization conductivity which is frequency dependent and weakly temperature-dependent and is equal to  $A\omega^s$ ,  $A$  is a constant that depends on temperature and composition and  $s$  is the frequency exponent that can take the value range of  $0 < s < 1$ . The frequency exponent  $s$  is very important in investigating the dominant electrical conductivity mechanism for the studied material [17, 19].

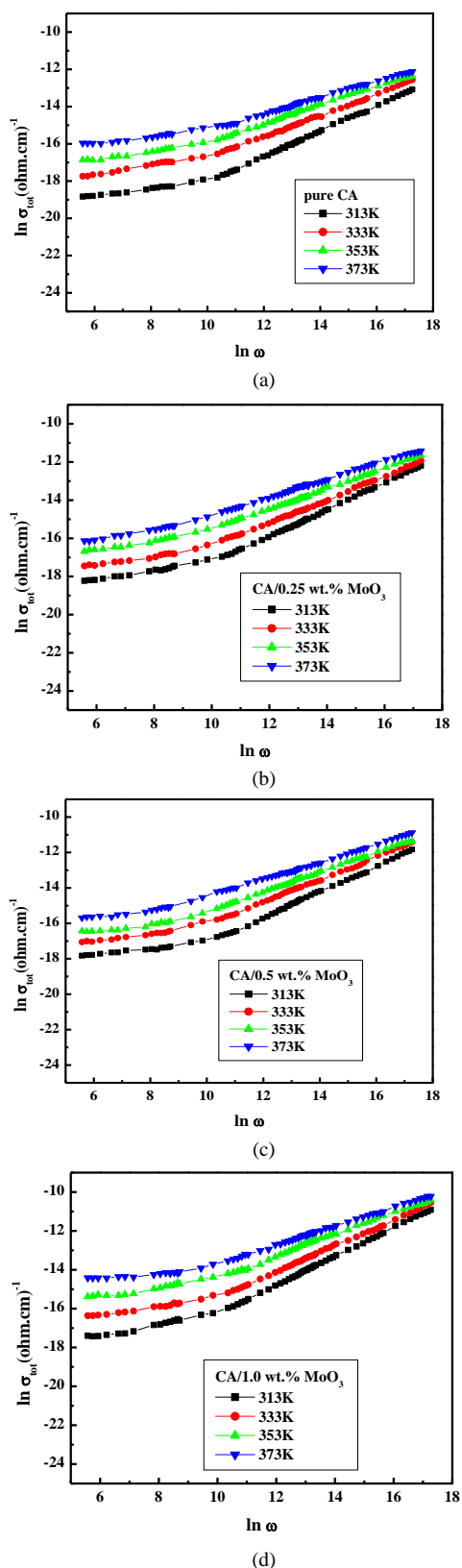
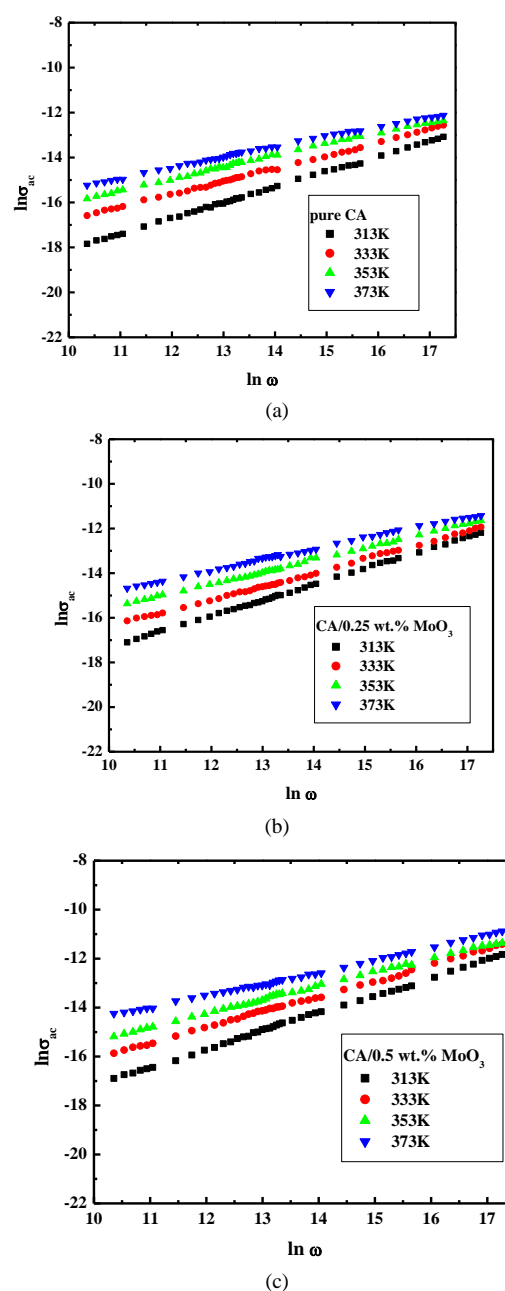


Fig. 1. Frequency dependence of total conductivity  $\sigma_{tot}(\omega)$  for (a) pure CA, (b) CA with 0.25 wt.%  $\text{MoO}_3$ -NPs (c) CA with 0.5 wt.%  $\text{MoO}_3$ -NPs and (d) CA with 1.0 wt.%  $\text{MoO}_3$ -NPs at different temperatures.

Ac conductivity is calculated for CA with different concentration of  $\text{MoO}_3$ -NPs from total conductivity by using equation (1). The values of the frequency exponent,  $s$ , is calculated from the slope of the straight lines of  $\ln \sigma_{ac}$  versus  $\ln(\omega)$  which is illustrated in figure 2 (a, b, c and d) as a function of temperature. As found in figure 2 (a, b, c & d). The ac conductivity was found to increase upon adding  $\text{MoO}_3$ -NPs and then increased upon increasing its concentration which can be attributed to that the metal oxide nanoparticle gets closer to each other as its concentration increase and make a conduction network which make the motion of charge carrier getting easier within the polymer matrix [20].



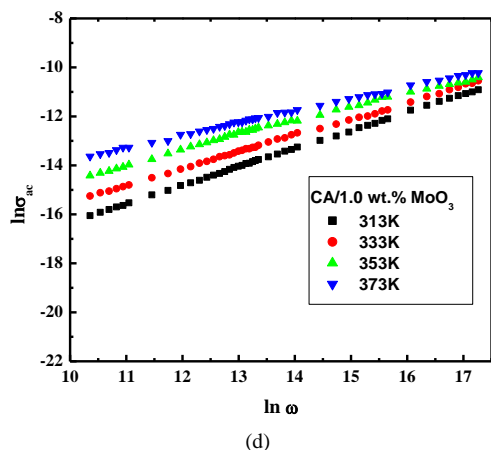


Fig. 2. Frequency dependence of AC conductivity  $\sigma_{ac}(\omega)$  for (a) pure CA, (b) CA with 0.25 wt.% MoO<sub>3</sub>-NPs (c) CA with 0.5 wt.% MoO<sub>3</sub>-NPs and (d) CA with 1.0 wt.% MoO<sub>3</sub>-NPs at different temperatures.

The value of  $s$  was calculated from the slope of the straight-line curve of  $\ln \sigma_{ac}$  versus  $\ln \omega$ . It is observed that the value of  $s$  for pure CA decreases with increasing the temperature from 0.66 to 0.45 which is in a good agreement with the previous result of pure CA [12]. Correlated barrier hopping model (CBH) was found to be the most suitable mechanism to describe the AC conductivity of CA in the studying range of temperature [21]. The value of frequency exponent  $S$  was found also to decrease with increasing the temperature for CA with different concentration of MoO<sub>3</sub>-NPs as it decrease from 0.71 to 0.48, 0.73 to 0.49 and 0.75 to 0.5 for MoO<sub>3</sub>-NPs concentration of 0.25 wt.% , 0.5 wt.% and 1.0 wt.% respectively which indicate that also CBH model is also the dominant mechanism for the blended samples. The variation of the frequency exponent  $s$  with temperature for CA with different concentration of MoO<sub>3</sub>-NPs is shown in fig.3.

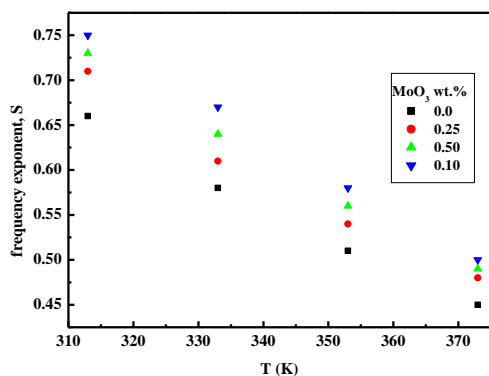


Fig. 3. Variation of frequency exponent  $s$  with temperature for CA with different concentration of MoO<sub>3</sub>-NPs

According to Elliott's CBH model, the electrical conductivity  $\sigma_{ac}$  due to bipolaron hopping to a first approximation is given by [21]:

$$\sigma_{ac} = (\pi^2 N^2 / 24) (8e^2 / \epsilon W_m)^6 (\omega^s / \tau_0^{1-s}) \quad (2)$$

where  $\epsilon$  is the dielectric constant of the material,  $e$  is the electronic charge,  $\tau_0$  is the effective relaxation time which expected to have a value of the order of an inverse phonon frequency ( $\approx 10^{-13}$  s) and  $W_m$  is the maximum barrier height over which the electrons hop energy gap between valence band " $\pi$ -band" and conduction band " $\pi^*$ -band" and is given by:

$$s = 1 - \frac{6k_B T}{W_m} \quad (3)$$

The value of  $W_m$  can be calculated from the slope of the straight-line fitting of the relation between  $T$  vs  $1-s$  and it was reported that  $W_m$  is equal to the band gap  $E_g$  for the material of conduction by bipolaron hopping. For the case of single polaron transport, the value of  $W_m$  in the CBH mechanism is equal to one quarter of  $E_g$  [21, 22]. In our case the value of  $W_m$  differ from the value of the energy gap calculated in our previous work [15] may be owing to many factors were not taken into consideration in CBH model such as; the structure characteristics of the material such as the average grain size, orientation, defect distribution, phase content, and charge carriers density. The values of  $W_m$  for CA with different concentration of MoO<sub>3</sub>-NPs is shown in table (1).

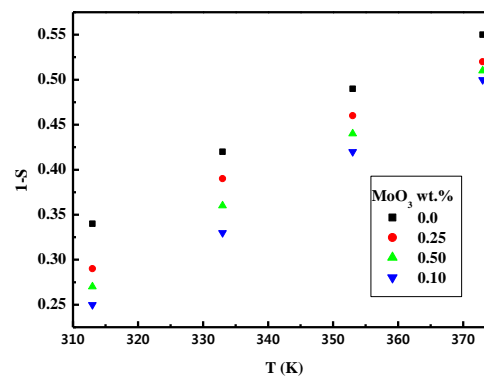


Fig. 4. Variation of maximum barrier height  $W_m$  with temperature for CA with different concentration of MoO<sub>3</sub>-NPs

Table 1. The variation of maximum barrier height  $W_m$  with MoO<sub>3</sub>-NPs concentration

Wt% MoO <sub>3</sub>	$W_m$ (eV)
0	0.2
0.25	0.14
0.50	0.13
1.00	0.11

The temperature dependence of  $\sigma_{ac}$  is represented by the well-known Arrhenius equation:

$$\sigma_{ac} = \sigma_0 \exp\left(\frac{\Delta E_{ac}}{k_b T}\right) \quad (4)$$

Where,  $\sigma_0$  is a pre-exponential factor and  $\Delta E_{ac}$  is the thermal activation energy for ac conduction. Activation energy for CA with different concentration of MoO<sub>3</sub>-NPs was determined from the slope of the relation between  $1000/T$  vs  $\ln \sigma_{ac}$  as shown in Fig. 6 (a,b,c,d).

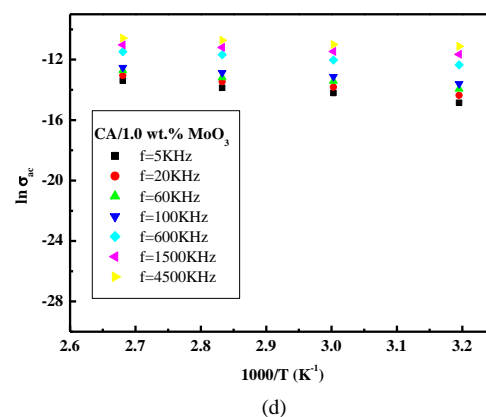
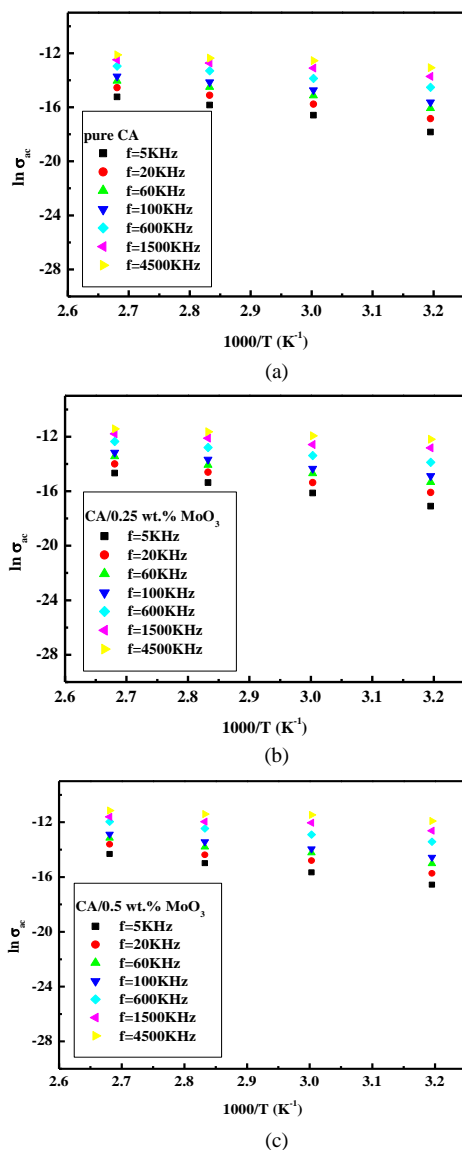


Fig. 5. Variation of AC conductivity  $\sigma_{ac}(\omega)$  with temperature for (a) pure CA , (b) CA with 0.25 wt.% MoO<sub>3</sub>-NPs (c) CA with 0.5 wt.% MoO<sub>3</sub>-NPs and (d) CA with 1.0 wt.% MoO<sub>3</sub>-NPs at different frequencies.

Figure 6 represent the thermal activation energy as a function of frequency which indicate that the activation energy decreases by increasing frequency in the range (5 KHz–4.5 MHz) which attributed to the increase in frequency which improve the electronic jumps between localized states and therefore the activation energy decreases with increasing frequency which also indicate that the hopping conduction is the dominant mechanism [23].

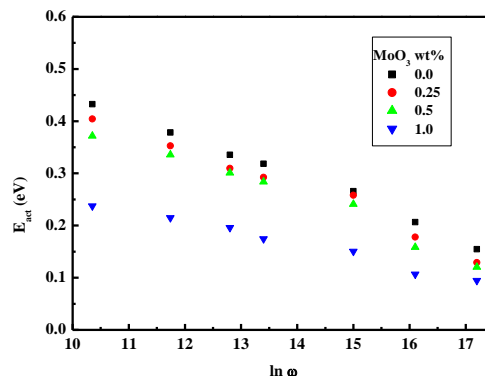


Fig. 6. Activation energy  $E_{ac}$  with frequency for CA with different concentration of MoO<sub>3</sub>-NPs

### Dielectric properties

The variations of real and imaginary parts of complex dielectric constant at different temperatures are analyzed by dielectric dispersion studies. The dielectric constant is accompanied with the polarization of the material under the influence of AC field [24]. The frequency dependence of the real part of the dielectric constant  $\epsilon'(\omega)$  at different temperatures for CA with different concentration of MoO<sub>3</sub>-NPs is shown in figure.7 (a, b, c and d). The figure shows a relatively high dielectric constant at low frequency which is caused by interfacial

polarization as a result of the orientation of polar group C-OCOCH<sub>3</sub> with varying electric field [13]. This dielectric constant is observed to decrease with increasing frequency reached a constant value at high frequency which can be attributed to that the polar group have sufficient time to align with the field at low frequency before it changes direction. At very high frequencies the dipoles do not have time to align before the field changes direction. At intermediate frequencies, the dipoles move but have not completed their movement before the field changes direction and they must realign with the changed field. This behavior can be explained by the Maxwell–Wagner–Sillars process [25]. It was observed from the figure that dielectric constant increase with increasing MoO<sub>3</sub>-NPs which is due to the enhanced polarization occurs as a result of the dipole–dipole interaction between the polymer and metal oxide nanoparticles. Also, the efficient interfacial interaction between the metal oxide nanoparticles and the polymer drive to the uniform conformation of the macromolecular chain of polymer, which is also responsible for the increasing of dielectric constant value of the blend [26].

As shown in figure dielectric constant for all samples was observed to increase with increasing the temperature which can be occurred due to that at low temperature segmental motion of polymer chain is practically freeze and will keep low dielectric constant but when the temperature increase, the intermolecular forces between polymer chain will be broken which will increase the segmental motion [25, 27].

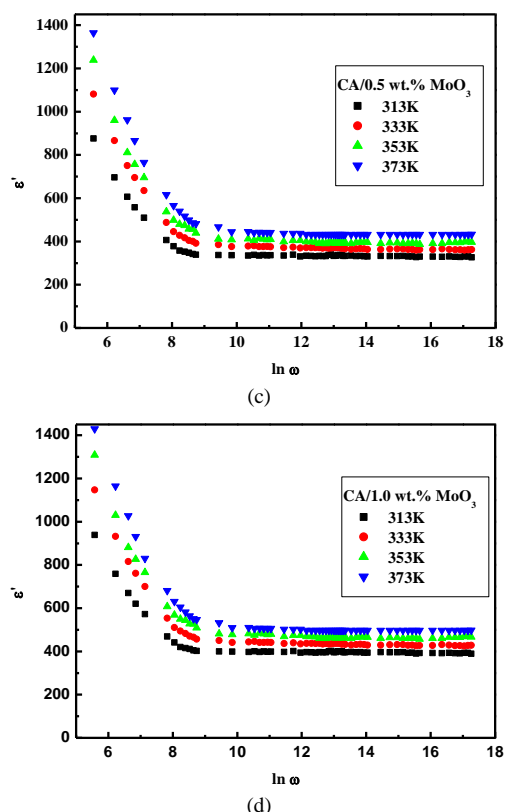
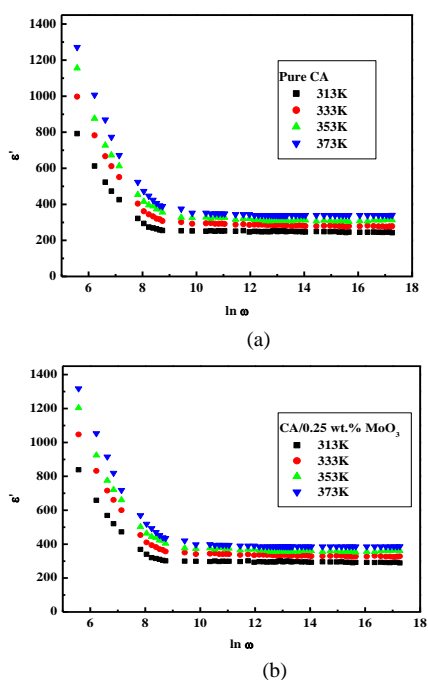
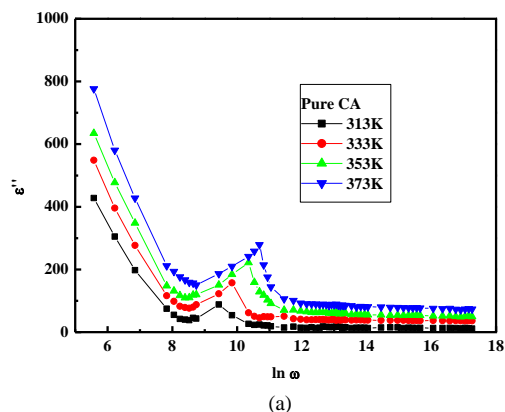


Fig. 7. Frequency dependence of dielectric constant  $\epsilon'(\omega)$  for (a) pure CA, (b) CA with 0.25 wt.% MoO<sub>3</sub>-NPs (c) CA with 0.5 wt.% MoO<sub>3</sub>-NPs and (d) CA with 1.0 wt.% MoO<sub>3</sub>-NPs at different temperatures.

Figure 8 (a, b, c & d) represent the variation of dielectric loss  $\epsilon''(\omega)$  as a function of  $\ln \omega$ . The figure shows a relaxation process for all samples. The relaxation peak for CA was previously obtained [13]. It is also observed that the peak frequency was shifted to higher frequencies with an increase in temperature. This characteristic suggests the existence of relaxation dipole in all samples.



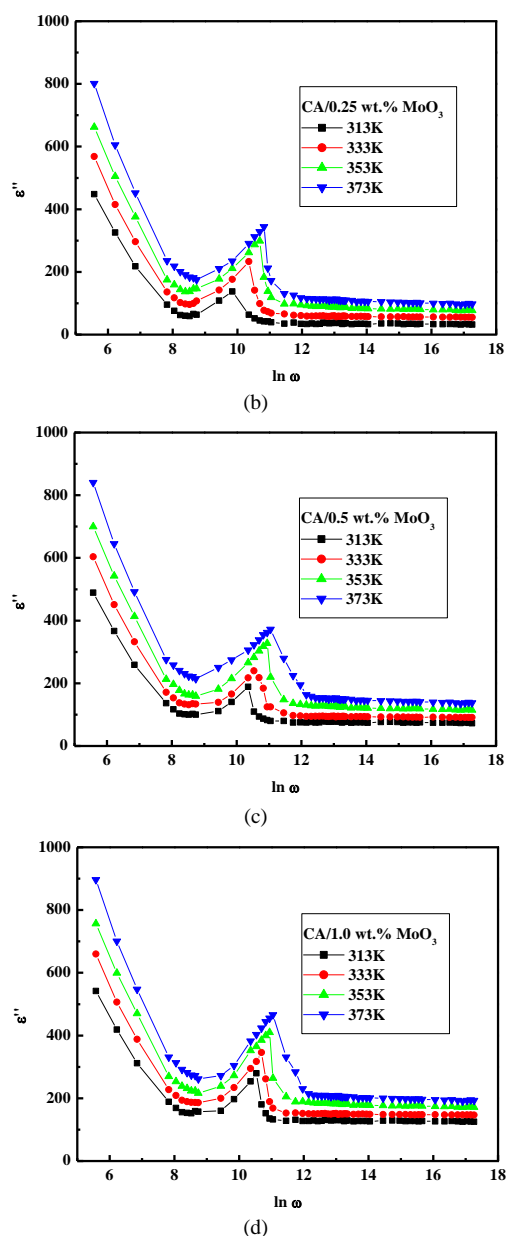


Fig. 8. Frequency dependence of dielectric loss  $\epsilon''(\omega)$  for (a) pure CA, (b) CA with 0.25 wt.%  $\text{MoO}_3$ -NPs (c) CA with 0.5 wt.%  $\text{MoO}_3$ -NPs and (d) CA with 1.0 wt.%  $\text{MoO}_3$ -NPs at different temperatures.

The activation energies of relaxation are calculated from the relaxation peak of dielectric loss in figure 8 according to the following equation [28]:

$$\omega_m = \omega_0 \exp\left(\frac{\Delta E_{ac}}{k_b T}\right) \quad (5)$$

Where  $\omega_m$  is the frequency at the relaxation peak;  $\omega_0$  is a constant. The activation energy of relaxation is calculated from the slope of the straight-line fitting of the relation between  $\ln \omega_m$  and  $1000/T$ . The relaxation activation energy was observed to decrease with increasing  $\text{MoO}_3$ -NPs concentration which is shown in the onset figure.

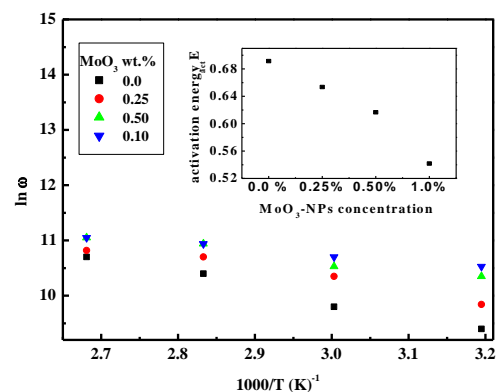


Fig. 9. Temperature dependence of the frequency at the maximum dielectric loss  $\epsilon''(\omega)$  of CA with different concentration of  $\text{MoO}_3$ -NPs.

#### 4. Conclusions

This work aimed to investigate the effect on ac conductivity and dielectric properties of pure cellulose acetate when blending with different concentration of Molybdenum Trioxide nanoparticles. The AC conductivity of the polymer was observed to increase by adding the nanoparticle and again increase with increasing its concentration. It was investigated that the Correlated Barrier Hopping model is the dominant mechanism in studying the AC conductivity of CA with different concentration of  $\text{MoO}_3$ -NPs. Activation energy was calculated and observed to decrease with increasing  $\text{MoO}_3$ -NPs concentration. The dielectric constant continuously decreased with an increase in frequency and reached a constant value at higher frequency which explained by the Maxwell–Wagner–Sillars process. The dielectric constant was observed to be higher at low frequency for all samples due to interfacial polarization. Dielectric loss was observed to increase with increasing  $\text{MoO}_3$ -NPs concentration which is due to enhancing the polarization by dipole-dipole interaction. A peak was observed in Dielectric loss curve in all samples due to the existence of relaxation process. Therefore, this study shows that the enhancing in ac conductivity and dielectric property in the blended film which make them as a promising material which can be used in various applications such as electromagnetic shielding, sensors and other nan electronic devices.

#### 5. References

- [1] Ramesan M. T., Varghese M., Periyat P., Silver- doped zinc oxide as a nanofiller for development of poly (vinyl

- alcohol)/poly (vinyl pyrrolidone) blend nanocomposites, *Advances in Polymer Technology*, 37, 137–143 (2018).
- [2] Mohiuddin M., Kim H.-C., Kim S.-Y., Kim J., Transparent and flexible haptic array actuator made with cellulose acetate for tactile sensation, in *Nanosensors, Biosensors, and Info-Tech Sensors and Systems 2014*, International Society for Optics and Photonics, 9060, 906017(2014).
- [3] Fotie G., Limbo S., Piergiovanni L., Manufacturing of Food Packaging Based on Nanocellulose: Current Advances and Challenges, *Nanomaterials*, 10, 1726 (2020).
- [4] Yu D.-G., Yu J.-H., Chen L., Williams G. R., Wang X., Modified coaxial electrospinning for the preparation of high-quality ketoprofen-loaded cellulose acetate nanofibers, *Carbohydrate polymers*, 90, 1016–1023 (2012).
- [5] Alsaif M. M. Y. A., Latham K., Field M. R., Yao D. D., Medehkar N. V., Beane G. A., Kaner R. B., Russo S.P., Ou J. Z., Kalantar-zadeh K. Tunable plasmon resonances in two-dimensional molybdenum oxide nanoflakes, *Advanced Materials*, 26, 3931–3937 (2014).
- [6] Balendhran S., Walia S., Alsaif M., Nguyen E. P., Ou J. Z., Zhuiykov S., Sriram S., Bhaskaran M., Kalantar-zadeh K., Field effect biosensing platform based on 2D  $\alpha$ -MoO<sub>3</sub>, *ACS Nano*, 7, 9753–9760, (2013).
- [7] Chen Y.-J., Gao X. M., Di X. P., Ouyang Q. Y., Gao P., Qi L. H., Li C. Y., Zhu C., Porous iron molybdate nanorods: in situ diffusion synthesis and low-temperature H<sub>2</sub>S gas sensing, *ACS applied materials and interfaces*, 5, 3267–3274 (2013).
- [8] Wang Y., Zhang X., Luo Z., Huang X., Tan C., Li H., Zheng B., Li B., Huang Y., Yang J., Zong Y., Liquid-phase growth of platinum nanoparticles on molybdenum trioxide nanosheets: an enhanced catalyst with intrinsic peroxidase-like catalytic activity, *Nanoscale*, 6, 12340–12344 (2014).
- [9] Wongkrua P., Thongtem T., Thongtem S., Synthesis of h- and  $\alpha$ -MoO<sub>3</sub> by refluxing and calcination combination: Phase and morphology transformation, photocatalysis, and photosensitization, *Journal of Nanomaterials*, 2013, (2013).
- [10] Ikada E., Sugimura T., Aoyama T., Watanabe T., Dielectric properties of oligomers: 4. Dielectric properties of vinyl acetate and methyl methacrylate oligomers, *Polymer*, 16, 101–104 (1975).
- [11] Ahmad-Fouad Basha M., Morsi Mohamed Morsi R., Spectroscopic, electrical, and relaxor-like properties of cellulose acetate–erbium (III) chloride composite films, *Journal of Applied Polymer Science*, 134, 1–10, (2017).
- [12] Sharma A. K., Ramu C., Dielectric Behaviour of Iron-Doped Cellulose Acetate Films, *Polymer international*, 29, 213–217 (1992).
- [13] Rajesh K., Crasta V., Kumar N. B. R., Shetty G., Effect of ZnO nanofiller on dielectric and mechanical properties of PVA/PVP blend, in *AIP Conference Proceedings*, 2162, 20096 (2019).
- [14] Rajesh K., Crasta V., NB R. K., Shetty G., Sangappa Y., Kudva J., Vijeth H., Effect of MoO<sub>3</sub> nanofiller on structural, optical, mechanical, dielectric and thermal properties of PVA/PVP blend, *Mater. Res. Innov.*, 24, 270–278 (2020).
- [15] Ezzat D., Mahmoud A. A., El-nahhas M., Elhaes H., Effect of ZnO Concentration upon the Structural Properties of Cellulose Acetate, *Middle East Journal of Applied Sciences*, 5, 64–72, (2015).
- [16] El-Nahass M. M., Metwally H. S., El-Sayed H. E. A., Hassanien A. M., Electrical conductivity and dielectric relaxation of bulk iron (III) chloride tetraphenylporphyrin, *Materials Chemistry and Physics*, 133, 649–654 (2012).
- [17] Jonscher A. K., The ‘universal’ dielectric response, *Nature*, 267, 673–679 (1977).
- [18] El-Nahass M. M., Atta A. A., Kamel M. A., Huthaily S. Y., AC conductivity and dielectric characterization of synthesized pN, N dimethylaminobenzylidenemalononitrile (DBM) organic dye, *Vacuum*, 91, 14–19 (2013).
- [19] Chen R. H., Chang R. Y., Shern S. C., Dielectric and AC ionic conductivity investigations in K<sub>3</sub>H (SeO<sub>4</sub>)<sub>2</sub> single crystal, *Journal of Physics and Chemistry of Solids*, 63, 2069–2077 (2002).
- [20] Sharma K., Kumar V., Kaith B. S., Kalia S., Swart H. C., Conducting polymer hydrogels and their applications, in *Conducting Polymer Hybrids*, Springer, 193–221(2017).
- [21] Elliott S. R., AC conduction in amorphous chalcogenide and pnictide semiconductors, *Advances in physics*, 36, 135–217 (1987).
- [22] Elliott S. R., A theory of ac conduction in chalcogenide glasses, *Philosophical Magazine*, 36, 1291–1304 (1977).
- [23] Bhatnagar V. K., Bhatia K. L., Frequency dependent electrical transport in bismuth-modified amorphous germanium sulfide semiconductors, *Journal of non-crystalline solids*, 119, 214–231 (1990).
- [24] El-Sayed S., Mahmoud K. H., Fatah A. A., Hassen A., DSC, TGA and dielectric properties of carboxymethyl cellulose/polyvinyl alcohol blends, *Physica B: Condensed Matter*, 406, 4068–4076 (2011).
- [25] Ahmad Z., Polymer dielectric materials, in *Dielectric material*, IntechOpen, (2012).
- [26] Sampreeth T., Al-Maghrabi M. A., Bahuleyan B. K., Ramesan M. T., Synthesis, characterization, thermal properties, conductivity and sensor application study of polyaniline/cerium-doped titanium dioxide nanocomposites, *Journal of Materials Science*, 53, 591–603 (2018).
- [27] Tareev B., Tareev B. M., *Physics of Dielectric Materials*, Mir Publ. Moscow, (1979).
- [28] Tripathy A., Das S. N., Bhuyan S., Choudhary R. N. P., Structural, Morphological and Electrical Impedance Spectroscopy of Bi<sub>2</sub>MnCdO<sub>6</sub> Double Perovskite Electronic Material, *Transactions on Electrical and Electronic Materials*, 20, 280–287 (2019).

## 6. Arabic abstract

تم استخدام طريقة الصب في تحضير عينات سيليلوز اسيتات المخلوطة بنسب تركيز 0.0, 0.5, 0.25 و 1 Wt. من نانو ثالث اكسيد الموليبدنيوم. تم دراسة بعض الدراسات الكهربائية وخصائص العزل باستخدام التيار المتردد والتي أظهرت ان الجزء الحقيقي من دالة العزل تزداد بزيادة درجة الحرارة في المدى من 313-373 درجة كلفينية ونقل ايضا بزيادة التردد في المدى من 42-5000000 هرتز وهذا السلوك يمكن دراسته باستخدام **Maxwell–Wagner–Sillar type polarization**. لوحظ ايضا ازدياد الجزء الحقيقي من دالة العزل بازدياد تركيز نانو ثالث اكسيد الموليبدنيوم. تم تعيين التوصيلية الكهربائية ووجد انها تزداد بزيادة درجة الحرارة وبزيادة تركيز نانو ثالث اكسيد الموليبدنيوم ويرسم العلاقة بين  $\log \sigma$  ومقلوب درجة الحرارة وجد انه هناك طاقة تنشيط والتي نقل قيمتها بزيادة التردد  $\omega$  المطبق على العينة كما وجد ان قيمة طاقة التنشيط نقل ايضا بزيادة تركيز نانو ثالث اكسيد الموليبدنيوم. و وجد كذلك ان التوصيلية الكهربائية تتبع القانون الأسى مع التردد المطبق عمليا للعلاقة  $\sigma_{ac} = A\omega^s$  حيث  $s$  بزيادة درجة الحرارة وبناء عليه تم تفسير انتقال حاملات الشحنة على أنها تنتقل بالقفز المتناسق عبر حواجز الطاقة.